Laser-Plasma Ion Acceleration

Andrea Macchi

CNR, Istituto Nazionale di Ottica, Adriano Gozzini lab., Pisa, Italy

Dipartimento di Fisica Enrico Fermi, Università di Pisa, Italy

ELISS22 Autumn School, ELI-NP, Magurele, Romania,
October 5, 2022

Reviews on ion acceleration (a selfish selection)

A. Macchi, M. Borghesi, M. Passoni,
Ion Acceleration by Superintense Laser-Plasma Interaction,
Rev. Mod. Phys. **85** (2013) 571

M. Borghesi, A. Macchi,
Laser-Driven Ion Accelerators: State of the Art and Applications,
in: *Laser-Driven Particle Acceleration Towards Radiobiology and Medicine* (Springer, 2016)

A. Macchi,
Laser-Driven Ion Acceleration,
in: *Applications of Laser-Driven Particle Acceleration* (CRC press, 2018), arXiv:1711.06443

A. Macchi,
A Superintense Laser-Plasma Interaction Theory Primer (Springer, 2013)
Chap.5 “Ion Acceleration” (for absolute beginners)

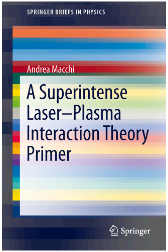

Other ion acceleration reviews

J. Schreiber, P. R. Bolton, K. Parodi,
"Hands-on" laser-driven ion acceleration: A primer for laser-driven source development and potential applications,
Rev. Sci. Instrum. **87** (2016) 071101

J.C. Fernández et al,
Fast ignition with laser-driven proton and ion beams,
Nucl. Fusion **54** (2014) 054006

H. Daido, M. Nishiuchi, A. S. Pirozhkov,
Review of Laser-Driven Ion Sources and Their applications,
Rep. Prog. Phys. **75** (2012) 056401

M. Borghesi et al,
Fast Ion Generation by High-Intensity Laser Irradiation of Solid Targets and Applications,
Fusion Science and Technology **49** (2006), 412

Artist's view . . .

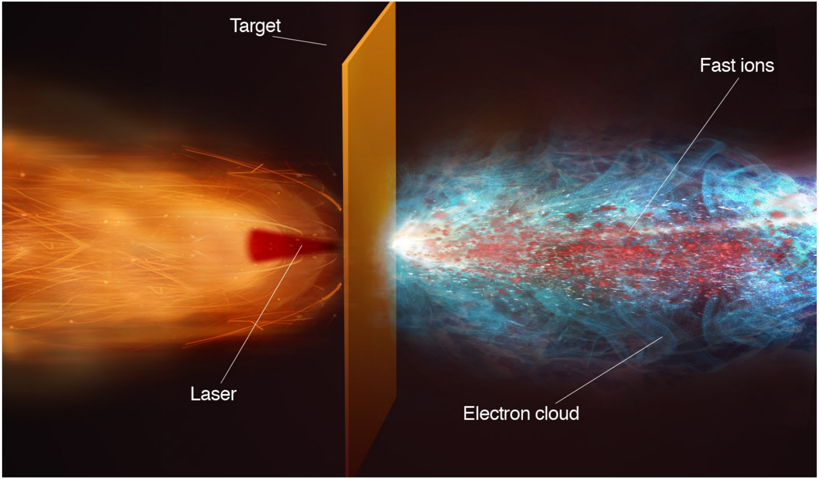

How it does (or should) work?

The “black box” hinders the acceleration mechanisms (not clear at time of discovery) The acceleration physics is of collective (cooperative, coherent) nature, based on self-consistent, non-linear plasma dynamics (complex and difficult to control)

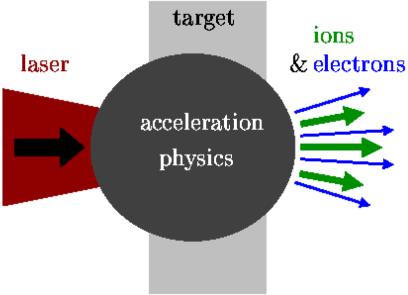

“*Is plasma involved? It can’t work*”
(Edward Teller on an early proposal of controlled fusion)

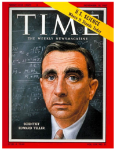

The vision of “coherent” acceleration: Veksler (1957)

“The principles of coherent acceleration of charged particles”
V. I. Veksler, At. Energ. **2** (1957) 525

- accelerating field on each particle proportional to the number of accelerated particles
- automatic synchrony between the particles and the accelerating field
- field localization in the region where the particles are
- acceleration of quasi-neutral bunches with large numbers of particles
- principles realized in laser-plasma acceleration of ions!

Several mechanisms (and acronyms) are at play

Example of a thick solid target with ion acceleration on both sides because of

- Target Normal Sheath Acceleration (TNSA)
- Radiation Pressure Acceleration (RPA)

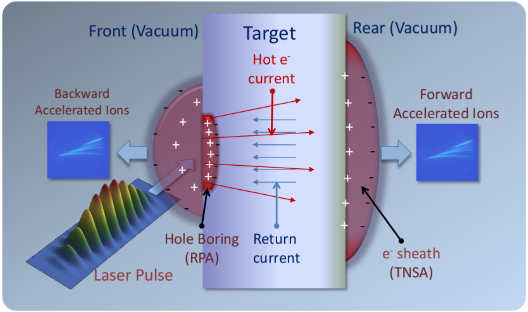

Different laser and target conditions activate new mechanisms: Relativistic Induced Transparency Acceleration (RITA), Collisionless Shock Acceleration (CSA), Magnetic Vortex Acceleration (MVA), Direct Coulomb Explosion (DCE), Break-Out Afterburner (BOA), . . .

. . . and complementary efforts are required

- laser development
- target engineering
- advanced diagnostics
- massive simulation
- theory

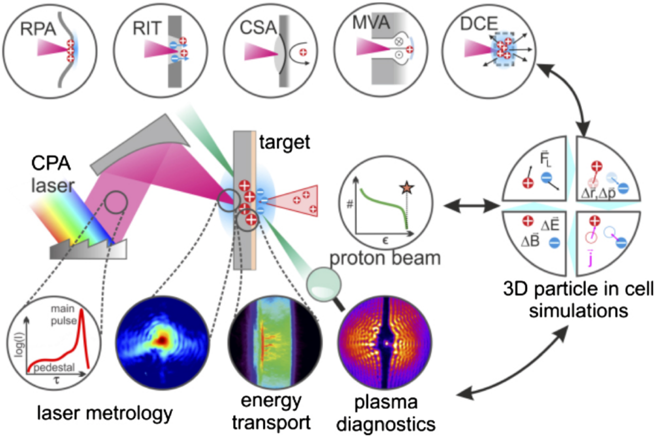

Figure: F. Albert et al, “2020 roadmap on plasma accelerators”, New J. Phys. **23** (2021) 031101

Multi-MeV protons from solid targets (2000–)

Up to 58 MeV protons observed at LLNL (Livermore) Petawatt

Snavely et al, PRL **85** (2000) 2945

Other observations:

Clark et al, PRL **84** (2000) 670

Maksimchuk et al, PRL **84** (2000) 4108

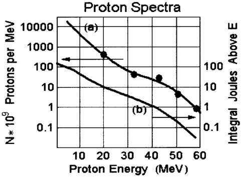

Protons (from H as either a target component or surface impurity) have been then observed in many laboratories and for different laser regimes

Figure: Borghesi et al,

Plasma Phys. Contr. Fus. **50** (2008) 124040

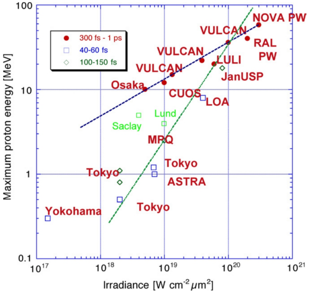

The race to higher proton energy

Highest cut-off energies to date, 2000–2018

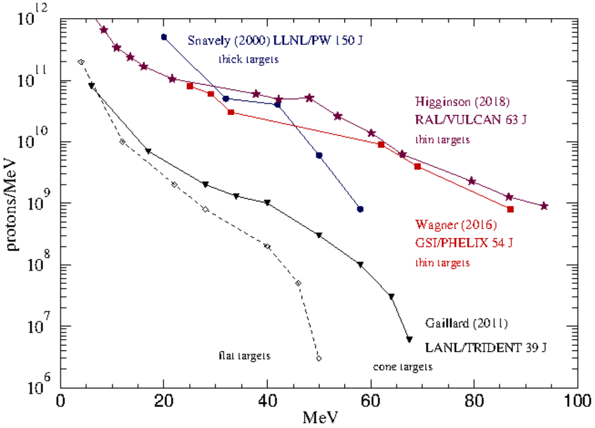

- Laser energy values given on target into focal spot (FWHM) (typically <50% of total available energy)
- pulse duration 0.5–1 ps
- different target types

Properties of laser-accelerated protons

- mostly broad energy spectra (exponential-like)
- large numbers - up to 2×10^{13} protons, ~kA current
  Snavely et al, PRL **85** (2000) 2945
- charge neutralization by comoving electrons ("plasma beam")
- good collimation with energy-dependent spread (angular aperture $\sim 10^\circ \div 30^\circ$)
- low emittance $\sim 4 \times 10^{-3}$ mm mrad
  (with cautious definition for broadband spectra)
  Nuernberg et al, Rev. Sci. Instrum. **80** (2009) 033301
- ultrashort duration near source:
  3.5 ± 0.7 ps measured with TARANIS laser (600 fs pulse)
  Dromey et al., Nature Comm. **7** (2016) 10642

What are those protons good for?

Energy deposition by ions in matter is strongly localized at the stopping point (Bragg peak)

$$\frac{d\mathscr{E}}{dx} \propto \frac{1}{\mathscr{E}^2}$$ (Coulomb scattering)

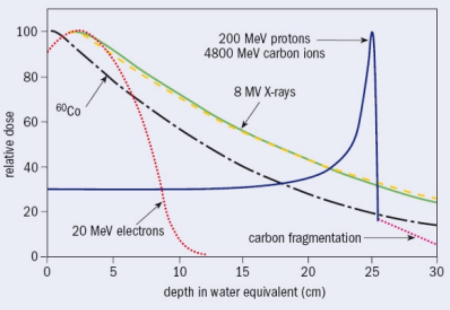

figure: Amaldi & Kraft, Rep. Prog. Phys. **68** (2005) 1861

(Foreseen) Applications:

- oncology: ion beam therapy
- diagnostic of materials
- production of warm dense matter
- triggering of nuclear reactions, isotope production
- ultrafast probing of electromagnetic fields

Does ultrafast-ultrahigh dose improve therapy?

frontiers in Oncology

REVIEW
published: 17 January 2020
doi: 10.3389/fonc.2019.01563

Ultra-High Dose Rate (FLASH) Radiotherapy: Silver Bullet or Fool's Gold?

Joseph D. Wilson[1†], *Ester M. Hammond*[1†], *Geoff S. Higgins*[1†] and *Kristoffer Petersson*[1,2*†]

[1] *Department of Oncology, The Oxford Institute for Radiation Oncology, University of Oxford, Oxford, United Kingdom,*
[2] *Radiation Physics, Department of Haematology, Oncology and Radiation Physics, Skåne University Hospital, Lund, Sweden*

Laser-driven ion accelerators may now test this regime exploting their unique properties

Proton probing of laser-plasma interactions

- charged beam:
  - ► field detection
- low emittance:
  - ► imaging capability
- laser driver:
  - ► easy synchronization
- broad spectrum:
  - ► time-of-flight arrangement
- short duration:
  - ► ultrafast resolution

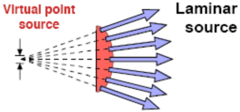

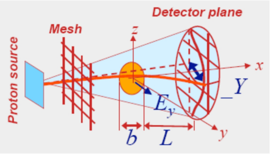

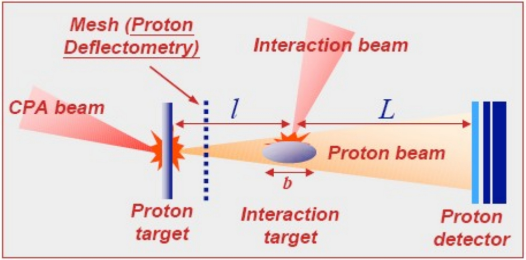

Achieving single-shot “movies”

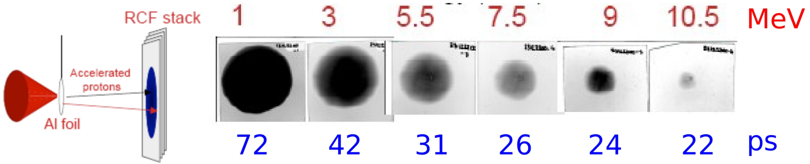

Time-of-flight arrangement: each RCF layer is a “snapshot” at a given proton energy ≡ probing time
(values for 1 mm flight distance)
Achievable resolution up to ~ 1 ps (depending on “crossing” time across field structures)

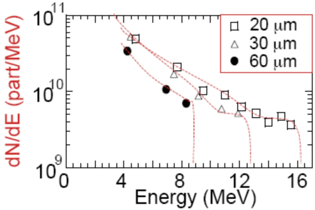

Higher proton energy yields higher resolution

Proton “image” formation

Small angle deflections by $\mathbf{E}$ and $\mathbf{B}$ create a dose modulation δn on RCF there producing an “image”
(with magnification M as for a virtual point source)

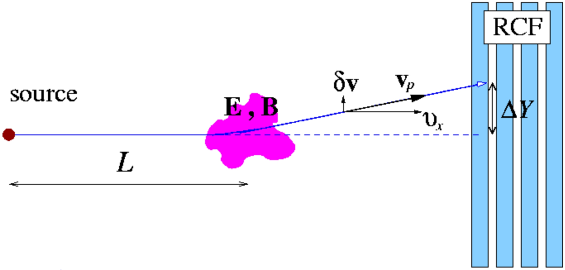

$$\Delta Y = |\delta\mathbf{v}|\Delta t \simeq \frac{eL}{2\mathcal{E}_p}\int(\mathbf{E}+\mathbf{v}_p\times\mathbf{B})_\perp dx$$

$$\frac{\delta n}{n_0} \simeq -\frac{1}{M}\nabla\cdot\Delta\mathbf{Y} \simeq \frac{-2\pi eLb}{\mathcal{E}_p M}\int_{-b/2}^{+b/2}\left(\rho - \frac{\mathbf{v}_p\cdot\mathbf{J}}{c^2}\right)dx$$

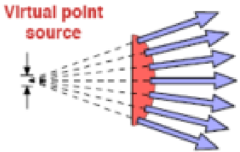

“Algorithm” for proton imaging analysis

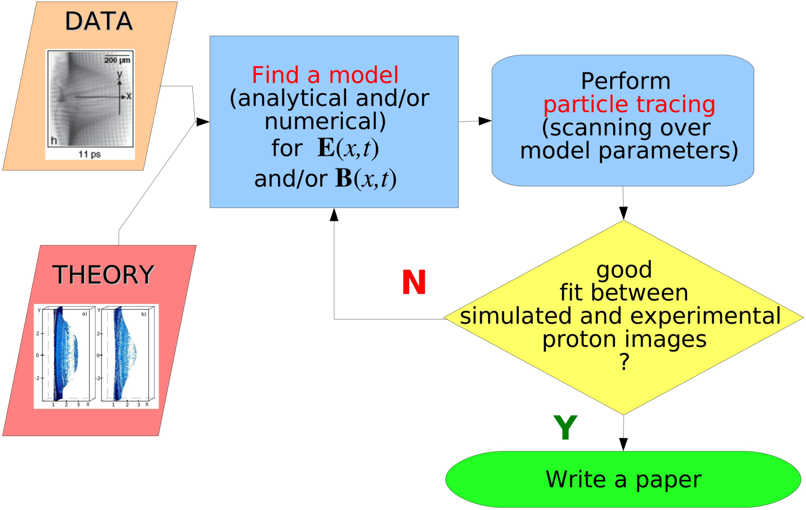

Where is the acceleration? The early debate

Snavely et al.: evidence of proton acceleration at the rear side of the target (opposite to the laser-irradiated front side)
Physics: plasma sheath formation by fast electrons generated at front side and escaping from the rear target side

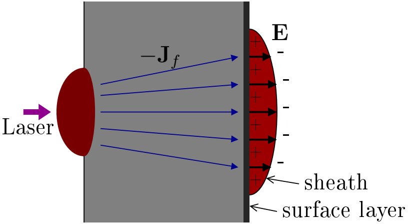

$\mathbf{J}_f$: fast electron current

The $\mathbf{E}$-field accelerates ions – mostly protons (from surface impurities) favored by initial position and highest Z/A)

Alternate interpretation: acceleration at the front side ...
(Clark et al. & Maksimchuk et al.)

Accelerated protons probe proton acceleration

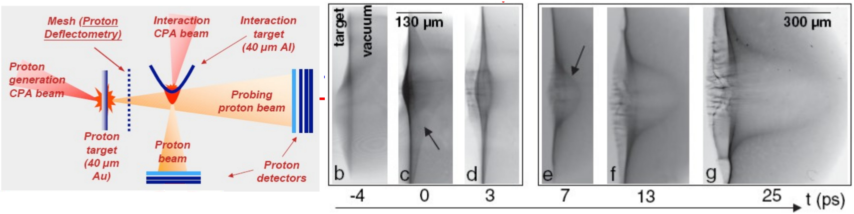

[Romagnani et al, PRL **95** (2005) 195001]

Bell-shaped fast moving electric field front observed at the rear side

Front position $x_f(t)$ is fitted by PIC electrostatic simulations of hot plasma expansion

$v_f = \frac{dx_f}{dt} \simeq 0.17c \longrightarrow \simeq$ 13 MeV protons

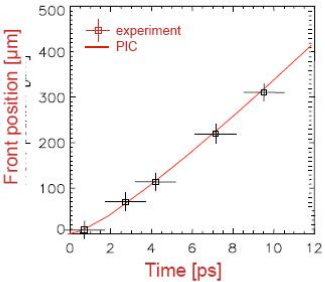

Magnetic fields at rear side

Purpose: detect magnetic fields "surrounding" the sheath region

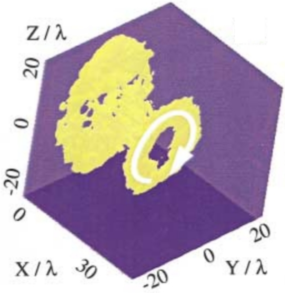

Technique: probing perpendicular to the target surface, (anti/)parallel to the symmetry axis of $\mathbf{B}$

[$\mathbf{B}$-field in 3D simulation - A.Pukhov, PRL **86**, 3562 (2001)]

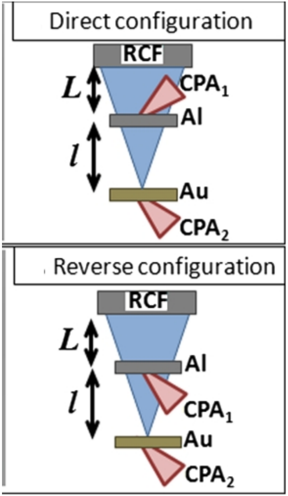

“Double-ring” pattern from magnetic field deflections

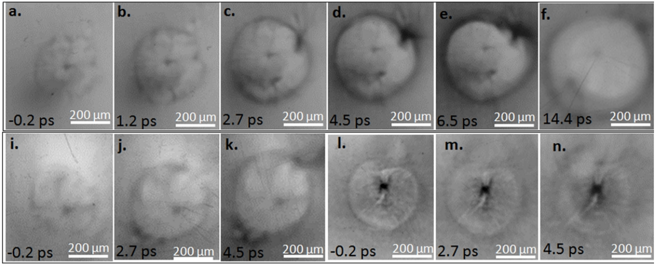

(**a-k**: *direct* config., **l-n**: *reverse* config.)

Front/rear side magnetic fields of opposite polarity cause focusing/defocusing of protons [G.Sarri et al, PRL **109**, 205002 (2012)]

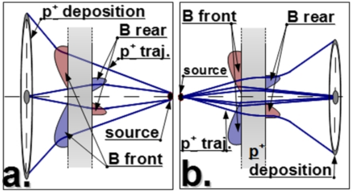

Temporal evolution of magnetic fields

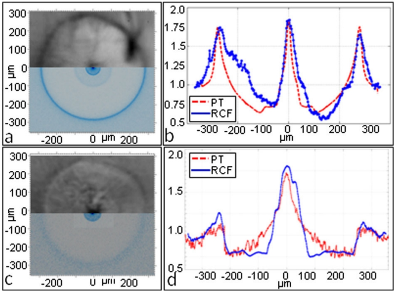

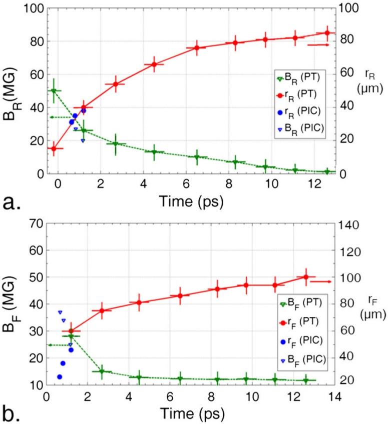

Measurements of $\mathbf{B} = \mathbf{B}(r, t)$ suggest that:

- sheath is magnetically confined in radial direction
- magnetic induction contributes significantly to $\mathbf{E}$

Transient sheath as a terahertz antenna

Escaping fast electrons yield a pulsed giant dipole antenna for unipolar ps pulses of current and **E**-field which drive the charge neutralization of the target

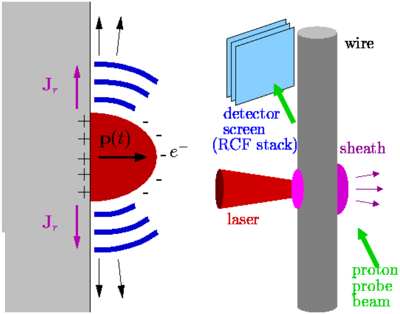

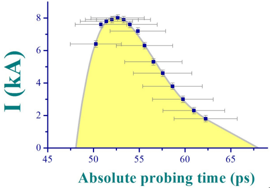

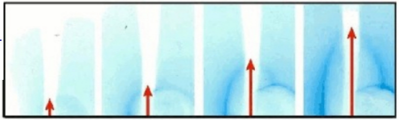

K. Quinn et al PRL **103** (2009) 194801

Efficient propagation along a folded wire

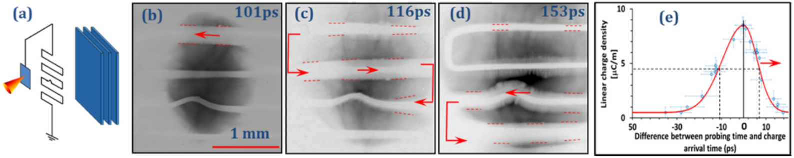

The unipolar pulse propagates as a surface wave with low losses and dispersion along ∼cm distances carrying ∼kA current and $\sim 10^8$ V m^{-1} electric field

Experiment on ARCTURUS laser (30 fs, $\gtrsim 10^{20}$ W cm^{-2}), Düsseldorf

S. Kar et al, Nature Comm. **7** (2016) 10792

Demonstrated also at QUB/TARANIS (600 fs, 10^{19} W cm^{-2})

LLNL/TITAN (600 fs, 2×10^{20} W cm^{-2}), RAL/VULCAN (1 ps, 3×10^{20} W cm^{-2})

H. Ahmed et al, Scient. Rep. **7** (2017) 10891; **11** (2021) 699

Application: steering of laser-accelerated protons

Traveling pulse along "coil":

synchronization with protons

longitudinal **E**-field for energy enhancement

radial **E**-field for collimation

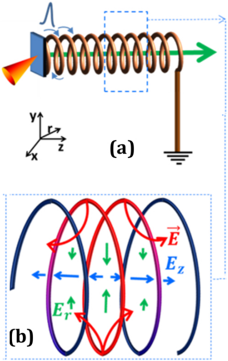

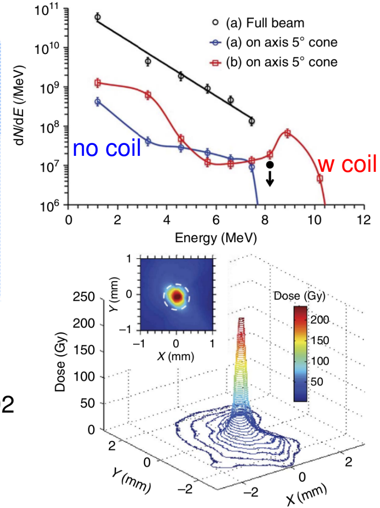

S. Kar et al, Nature Comm. **7** (2016) 10792
Satyabrata Kar,
"Beam focusing and accelerating system",
patent 20160379793 (2016)

Understanding Target Normal Sheath Acceleration

TNSA is the most "robust" and investigated regime so far

Although the sheath physics is highly complicated . . .

. . . reasonably simple models are needed to:

- infer scaling with laser & target parameters
- optimize performance

Basic "ingredients" of simple(st) model:

- fast electron generation
- sheath modeling

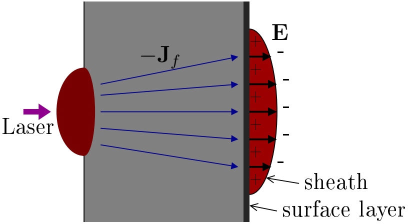

"*There are more things between cathode and anode that are dreamt in your philosophy*" (H. Raether)

Generation of “fast” electrons - 1

Short pulse interaction with solid targets

$$n_e \gg n_c = \frac{m_e \omega^2}{4\pi e^2} \text{ i.e. } \omega \ll \omega_p$$

ω_p plasma frequency, n_c cut-off or “critical” density

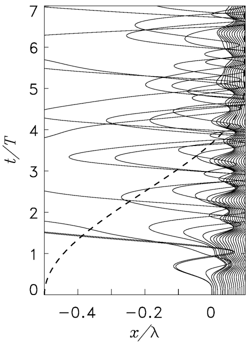

In the short gradient the laser-driven surface oscillations “break” and release energy to particles

Electrostatic simulation: trajectory self-intersection, *wavebreaking* and generation of “fast” electron bunches

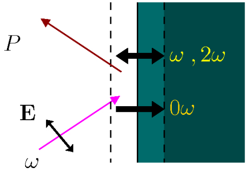

P-pol.: $\mathbf{E}$-driven, $\Omega = \omega$

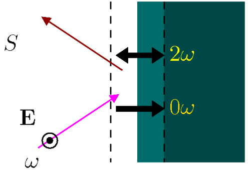

S-pol.: $\mathbf{v} \times \mathbf{B}$-driven, $\Omega = 2\omega$

Generation of “fast” electrons - 2

Single particle picture: oscillating forces drag electrons into the vacuum side and push them back in the plasma after an half-cycle
(strongly non-adiabatic motion)

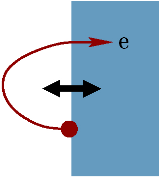

Popular definitions:

“Vacuum heating” or “Brunel effect” if $\mathbf{E}$-driven at rate ω

[Brunel, Phys. Rev. Lett. **59** (1987) 52; Phys. Fluids **31** (1988) 2714]

“$\mathbf{J}\times\mathbf{B}$” heating if $\mathbf{v}\times\mathbf{B}$-driven at rate 2ω

[Kruer & Estabrook, Phys. Fluids **28** (1985) 430]

Empirical “ponderomotive” scaling for fast electron temperature

$$T_{\rm f} = m_e c^2 \left((1 + a_0^2/2)^{1/2} - 1\right) \qquad a_0 = 0.85\left(\frac{I_L\lambda_L^2}{10^{18}\ \mathrm{Wcm^{-2}}\mu\mathrm{m}^2}\right)^{1/2}$$

"Elementary" TNSA modeling: static case

Assume fast electrons in Boltzmann equilibrium with density n_e and temperature T_e as the only parameters to evaluate sheath extension L_s and potential drop $\Delta\Phi$

$$L_s \simeq \lambda_D = (T_e/4\pi e^2 n_e)^{1/2}\,, \qquad \Delta\Phi \simeq T_e/e$$

Energy gain by a "test" ion in the static sheath:

$$\mathscr{E}_{\text{max}} = Ze\Delta\Phi \simeq ZT_e$$

⚠ : exact treatment yields

$$L_s \to \infty \qquad \Delta\Phi \to \infty$$

if Boltzmann's distribution is not "truncated" at high energy

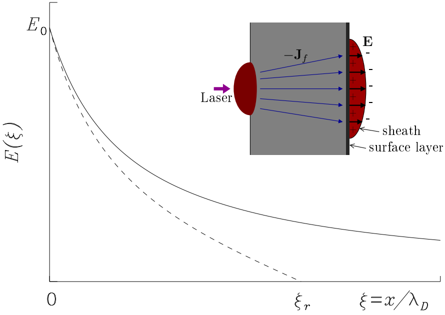

“Elementary” TNSA modeling: dynamic case

Plasma expansion model: isothermal rarefaction wave solution “patched” at the ion front where quasi-neutrality breaks down

$$c_s = \left(\frac{ZT_e}{m_i}\right)^{1/2} , \quad u_f \equiv u_i(x_f) = c_s[2\ln(\omega_{pi}t)+1] , \quad \mathscr{E}_{\max} = \frac{m_i}{2}u_f^2 \propto ZT_e$$

⚠: ion energy diverges due to infinite energy reservoir!
assume finite model (e.g thin foil expansion) with $T_e(t)$
assume finite acceleration time (extra patch)

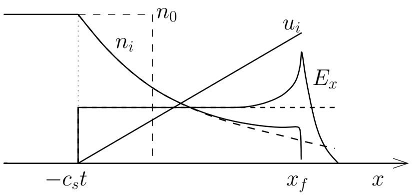

Charging and "truncation" by electron escape

- An isolated, warm plasma in "real" 3D space gets charged due to the escape of $N_{\rm esc}$ electrons with energy $> U_{\rm esc}$ (since the binding potential is limited)
  - For a simple spherical emitter of radius R having N_0 electrons at T_e:

$$N_{\rm esc} = N_0 \exp\left(-\frac{U_{\rm esc}}{T_e}\right) \qquad U_{\rm esc} = \frac{e^2 N_{\rm esc}}{R}$$

- Message: cut-off energy $U_{\rm esc}$ (hence $\mathscr{E}_{\rm max}$) depends on target density, size, ...

⚠: the system is neither steady nor in Boltzmann equilibrium, the target is neither isolated nor grounded, ...

Issues with fitting TNSA models

- "Elementary" modeling suggests a scaling of cut-off energy $\mathscr{E}_{\text{co}} \propto T_f \propto a_0 \propto I_L^{1/2} \quad (a_0 \gg 1)$
- Survey of experiments have suggested the scaling to be different for "long" (>ps) and "short" (<ps) pulses
- Fitting of data using theoretical (or semi-empirical) models is not conclusive because of:
  - large variation in data (mostly reported on log-log scale)
  - ambiguities of $\mathscr{E}_{\text{co}}$ as the most relevant quantity (value can be affected by finite instrumental resolution)
  - some "free" model parameters for what cannot be measured

A selection of short pulse results

Attempt to reduce the effect of different experimental conditions:

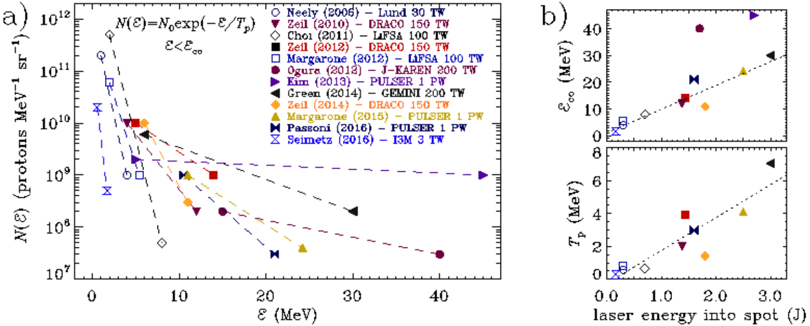

short pulses (25–40 fs) & solid targets (0.01–4.0 μm) & high contrast

calibrated exponential spectra $N_p(\mathcal{E}) = N_{p0}\exp(-\mathcal{E}/T_p)$

$I = (1-5)\times 10^{19}$ Wcm^{-2} (empty symbols)

$I = (0.3-2)\times 10^{21}$ Wcm^{-2} (**filled** symbols)

“Ultraclean” high-contrast pulses

Ionization shutters (“plasma mirrors”) yield pulse-to-prepulse intensity contrast $> 10^{11}$ $\longrightarrow$ sub-wavelength structuring is preserved until the short pulse interaction

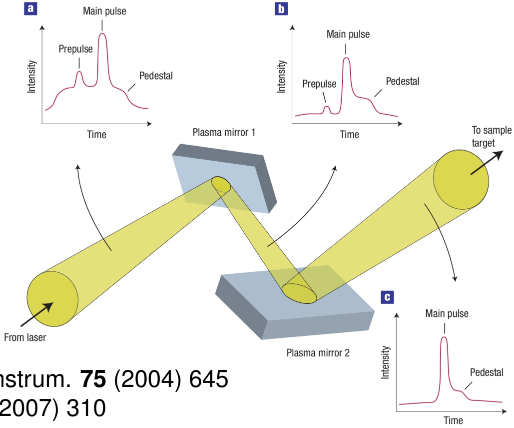

B. Dromey et al, Rev. Sci. Instrum. **75** (2004) 645
A. Levy et al, Opt. Lett. **32** (2007) 310
C. Thaury et al, Nature Physics **3** (2007) 424
figure from P. Gibbon, *ibid.* 369

A selection of short pulse results

Almost linear scaling of $\mathscr{E}$ & T_p with pulse energy

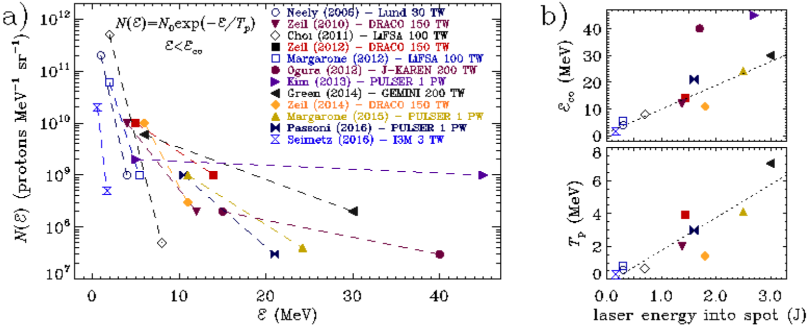

- Any TNSA model for the $\simeq 9$ MeV/J slope?
- Two “anomalous” results possibly in different regime?

Ogura (2012): relatively low contrast, Kim (2013): ultrathin 0.01 μm target

Engineered targets for enhanced TNSA

- low-average density layers (e.g. foam-covered targets)

  rationale: field enhancement as resonance $\omega_p \simeq \omega$ is approached

$\longrightarrow$ more energetic electrons

- mass-limited targets (e.g. isolated spheres)

  rationale: fast electron confinement in small volume

$\longrightarrow$ "hotter" sheath with higher field

- target with surface structuring

  rationale: laser coupling is sensitive to near– & sub–wavelength structures

$\longrightarrow$ higher absorption, faster electrons

- drawback: more complex targets, expensive fabrication, ...

Energy enhancement in “special” targets

Up to $\simeq 50\%$ cut-off increase w.r.t. to standard “flat” targets:

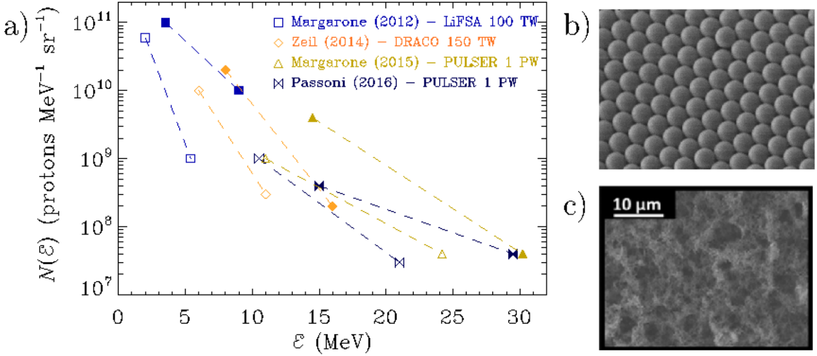

Zeil (2014): mass-limited foils
Margarone (2012, 2016): sub-μm spheres **(b)**
Passoni (2016): foam-covered targets **(c)**

FEM images

Grating-enhanced proton emission

CEA Saclay/SLIC laser: 28 fs, 5×10^{19} Wcm^{-2}

ultrahigh contrast $\sim 10^{12}$ enables use of periodically engraved targets (gratings)

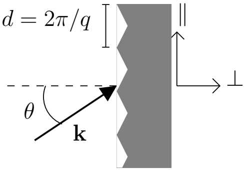

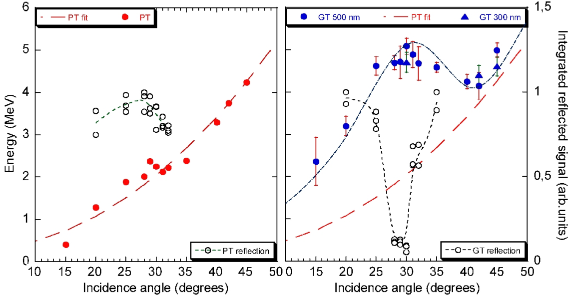

$$\sin\theta \simeq n\frac{\lambda}{d} - 1$$

resonant angle for surface plasma wave (SPW) excitation

$\longrightarrow$ reflectivity dip & $\sim$ 2.5X increase in proton energy with respect to “flat” targets [Ceccotti et al, PRL **111** (2013) 185001]

Electron heating & acceleration by SPW

SPW enhances EM field near the surface $\longrightarrow$ higher absorption & more energetic electrons

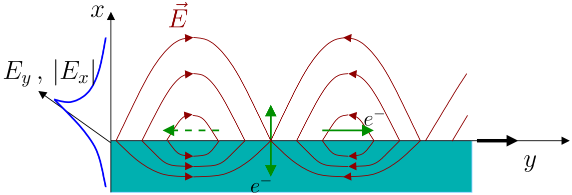

Transverse electric field (E_x) enhances "vacuum heating"
$\longrightarrow$ enhanced TNSA from fast electrons into the target

Longitudinal electric field (E_y)
+ phase velocity $v_f = \omega / k \lesssim c$
$\longrightarrow$ electrons are accelerated along the surface by "surfing" the SPW

Observation of “surfing” electrons

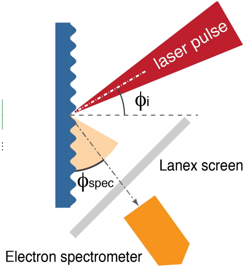

- collimated ($\simeq 20°$ cone) electron emission near the surface tangent ($\phi \simeq 2°$)
- multi-MeV energy ($\gg$ “ponderomotive” value)
- total charge up to $\simeq 650$ pC

L.Fedeli et al, PRL **116** (2016) 015001

G.Cantono et al, PoP **25** (2018) 031906

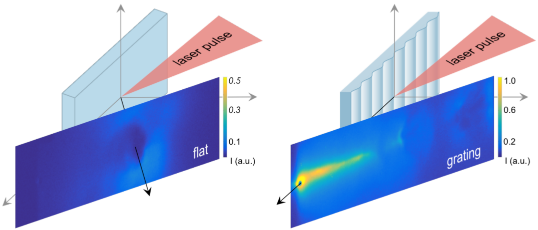

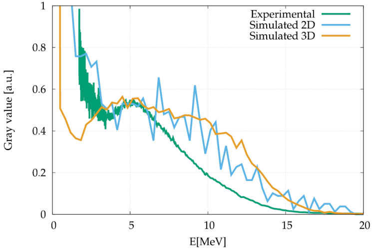

SPW-based “Peeler” Proton Acceleration

“A fs laser (red and blue) is incident on the edge of a micron-thick tape (grey) [. . .] Abundant electrons are trapped in the longitudinal potential well and accelerated by the SPW field”

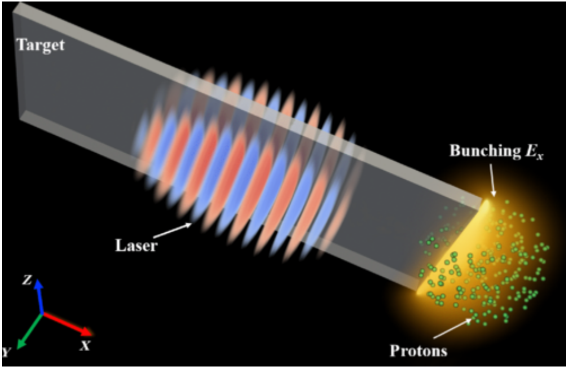

X.Shen, A.Pukhov, B.Qiao, Phys. Rev. X **11** (2021) 041002

SPW-based "Peeler" Proton Acceleration

"[...] at the rear edge a longitudinal bunching field is established (yellow). Protons (green dots) are simultaneously accelerated and leading to a highly monoenergetic beam."

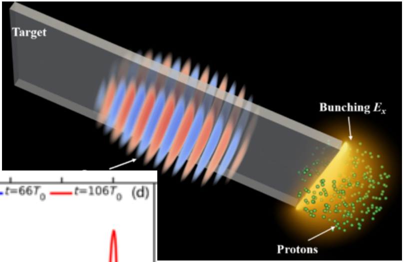

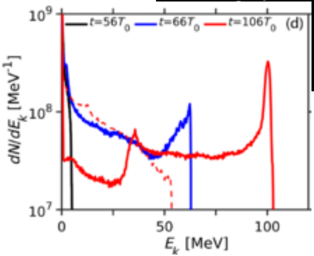

Pulse: 45 fs

7.8×10^{20} Wcm^{-2}

Target:

$n_e/n_c = 30$

$d = 50$ nm

X.Shen, A.Pukhov, B.Qiao, Phys. Rev. X **11** (2021) 041002

Origin of Monoenergetic Proton Spectra

TNSA: fast electrons are less than protons in the layer which screen the $\mathbf{E}$-field producing a sharp gradient

PEEL: protons are less than fast electrons and the space charge $\mathbf{E}$-field on the proton layer is spatially “smooth”.

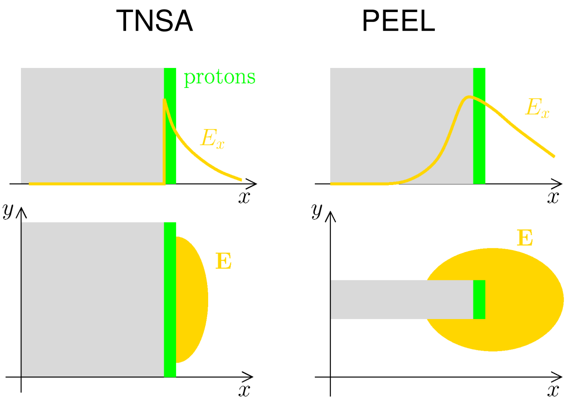

All protons experience almost the same field $\longrightarrow$ monoenergetic acceleration

A simulation campaign

Aim: test tolerance of "peeler" acceleration scheme with respect to grazing (non-parallel) & off-axis incidence (in view of scheduled experiments)

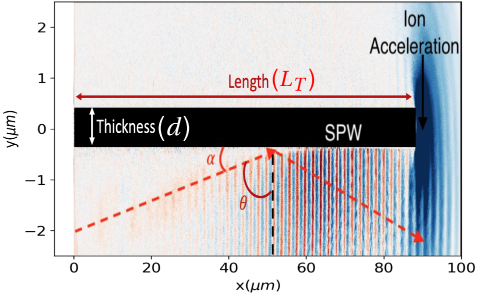

simulations by J. Sarma & A. McIlvenny (Queen's University Belfast)
PIC code EPOCH, 2D Cartesian geometry
$I = (0.34 - 7.8) \times 10^{20}\ \mathrm{Wcm}^{-2}$, 35 fs, $\lambda = 0.8\ \mu\mathrm{m}$, $a_0 = (5 - 19)$
$n_e = 1.7 \times 10^{23}\ \mathrm{cm}^{-3} = 100 n_c$, $d = 0.8\ \mu\mathrm{m}$, $L_T = (90 - 200)\ \mu\mathrm{m}$

Non-perfect alignment yields better results

Highest cut-off energy is reached for parallel incidence with "shifted" pulse ($\delta = 2.3\ \mu\text{m}$)
Slightly lower energy at grazing incidence ($\alpha = 1.5°$)

$I = 6 \times 10^{20}\ \text{Wcm}^{-2}$

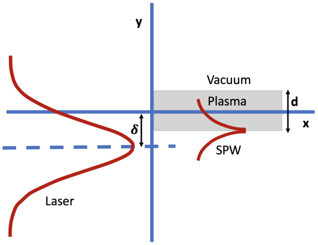

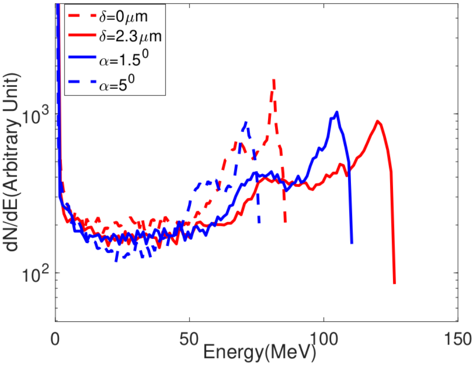

J.Sarma et al,
New. J. Phys. **24** (2022) 073023

Light Sail boosted by radiation pressure

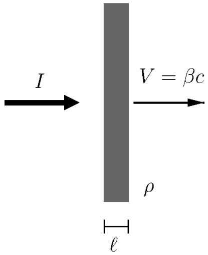

At normal incidence the total cycle-averaged $\mathbf{J} \times \mathbf{B}$ force per unit surface is $P = 2\dfrac{I}{c}$

EoM for a plane mirror of finite mass

$$\frac{\mathrm{d}(\gamma\beta)}{\mathrm{d}t} = \frac{2}{\rho \ell c^2} I\left(t - \frac{X}{c}\right) \frac{1-\beta}{1+\beta} \qquad \frac{\mathrm{d}X}{\mathrm{d}t} = \beta c$$

Analytical solution "observed" in simulations of thin foil acceleration at $\sim 10^{23}\ \mathrm{Wcm}^{-2}$

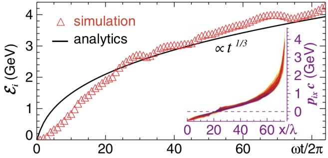

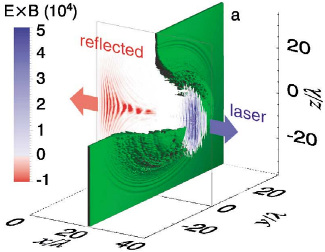

Esirkepov et al, PRL **92** (2004) 175003

Example: Coherent "Radiation Drag" Acceleration

Equations of motion for a particle (radius $a \ll \lambda$) undergoing Thomson Scattering of a plane EM wave ($P_{sc} = \sigma_T I$)

P_{sc}: scattered power

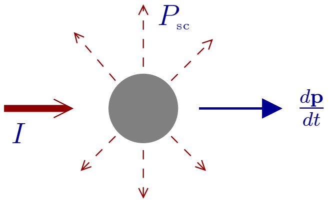

$$\frac{\mathrm{d}}{\mathrm{d}t'}(M\gamma' V') = \sigma_T \frac{I(t')}{c} \quad \text{(rest frame)}$$

$$\frac{\mathrm{d}}{\mathrm{d}t}(M\gamma V) = \sigma_T \frac{I(t_{rit})}{c} \frac{1 - V/c}{1 - V/c} \quad \text{(lab)}$$

For coherent scattering by a cluster with N ($\gg 1$) particles

$$M \rightarrow NM$$
$$P_{sc} \rightarrow N^2 P_{sc}$$
$$\sigma_T \rightarrow N^2 \sigma_T$$

$\longrightarrow$ N-fold increase in acceleration (Veksler, 1957)

Light Sail energy from conservation laws

Conservation of 4-momenta in "collision" between laser pulse and moving mirror (mass $M = \rho\ell$)

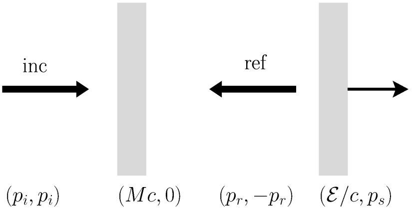

$$\begin{aligned} p_i + mc &= p_r + \mathscr{E}/c \\ p_i &= -p_r + p_s \end{aligned}$$

Using $\mathscr{E}^2 = M^2c^2 + p_s^2$ and $p_i = \int_0^\infty \frac{I(t')}{c}\mathrm{d}t' \equiv \frac{Mc}{2}\mathscr{F}$

energy $\frac{\mathscr{E}}{Mc^2} = \frac{\mathscr{F}^2}{2(\mathscr{F}+1)}$ $\left(\simeq \frac{\mathscr{F}^2}{2} \text{ for } \beta = \frac{p_s c}{\mathscr{E}} \ll 1\right)$

efficiency $\eta = \frac{\mathscr{E}}{p_i c} = \frac{2\beta}{1+\beta}$ $\longrightarrow$ 100% in the $\beta \to 1$ limit

Foreseen laser sailing . . .

R.Forward (1964)
G.Marx (1966)

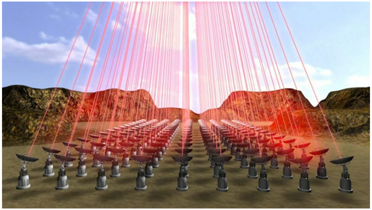

Breakthrough Starshot (2016)

breakthroughinitiatives.org

Critical analysis of (un)feasibility:

H.Milchberg, Phys. Today, 26 April 2016

Light Sail with extreme light on nanofoils

Energy/nucleon & efficiency from the 1D mirror model

(τ_p: laser pulse duration)

$$\mathscr{F} = \frac{2I\tau_p}{\rho\ell} = \frac{Z}{A}\frac{m_e}{m_p}\frac{a_0{}^2}{\zeta}\omega\tau_p \qquad \left(\zeta = \pi\frac{n_e}{n_c}\frac{\ell}{\lambda}\right)$$

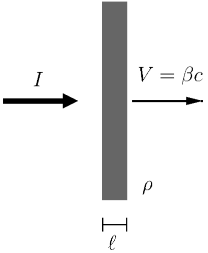

Optimal thickness $a_0 \simeq \zeta$ at threshold of relativistic transparency

$$\mathscr{E}_{\max} \simeq 2\pi^2 \frac{(m_e c)^2}{m_p}\left(\frac{Z}{A}\frac{c\tau_p}{\lambda}a_0\right)^2$$

$\ell \simeq 10$ nm , $I \simeq 1.6 \times 10^{21}$ W cm^{-2} ($a_0 = 22$) , $\tau_p = 40$ fs

$\longrightarrow$ $\mathscr{E}_{\max} \simeq 150$ MeV , $\eta \simeq 50\%$

Coherent motion of the sail $\longrightarrow$ mononergetic ion spectrum

A dream ion beam? ...

Transparency of ultrathin plasma foil

1D model with relativistic nonlinearity

$n_e(x) \simeq n_0 \ell \delta(x)$ (ℓ: foil thickness)

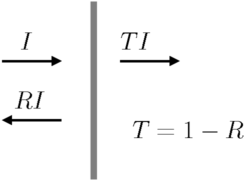

[V.A.Vshivkov et al, Phys. Plasmas **5** (1996) 2727]

Nonlinear reflectivity:

$$R \simeq \begin{cases} 1 & (a_0 < \zeta) \\ \dfrac{\zeta^2}{{a_0}^2} & (a_0 > \zeta) \end{cases} \qquad \zeta \equiv \pi \frac{n_0 \ell}{n_c \lambda}$$

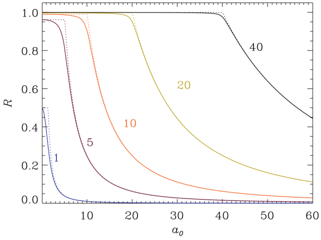

The transparency threshold $a_0 \simeq \zeta$ depends on areal density $n_0 \ell$

(note: it is *not* $n_e < n_c \gamma$ with $\gamma = (1 + a_0^2)^{1/2}$)

Suppress heating to make light pressure dominant

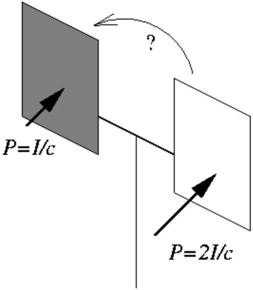

The "Optical Mill" (Crookes radiometer) rotates in the *opposite* way to that suggested by the imbalance of light pressure between white (reflecting) and black (absorbing) faces

$$P = (1+R)\frac{I}{c}$$

(white: $R \simeq 1$, black: $R \simeq 0$)

This is because the *thermal* pressure dominates due to stronger heating of the black face (in imperfect vacuum)
How to reduce heating in superintense laser interaction?

Circular polarization quenches heating

Radiation pressure must overcome the fast electrons pressure
Circular Polarization (CP) & normal incidence:
the 2ω component of the $\mathbf{v} \times \mathbf{B}$ force vanishes
$\rightarrow$ longitudinal oscillations and electron heating are suppressed

Ions respond smoothly to steady force: Radiation pressure dominates the interaction

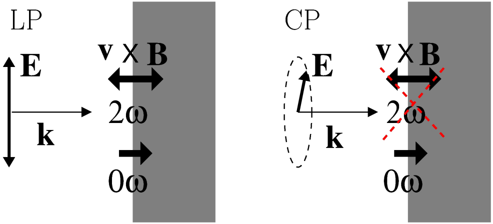

[Macchi et al, Phys. Rev. Lett. **95** (2005) 185003]

Fast electron generation: effect of polarization

1D simulations of laser interaction with solid-density plasma

density

phase space

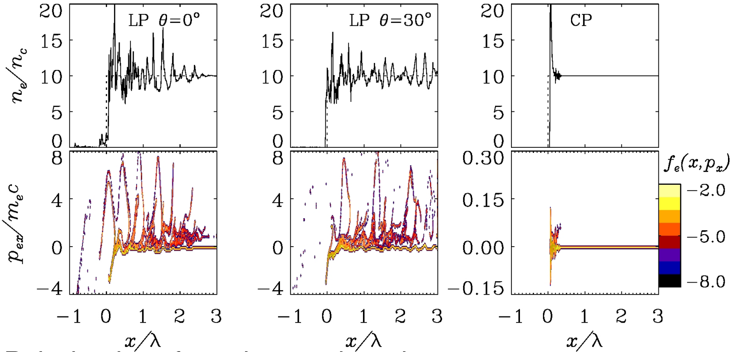

Linear Polarization: fast electron bunches at rate ω (for $\theta = 30°$, P-pol.) or 2ω (for $\theta = 0°$)

Circular Polarization at $\theta = 0°$: no fast electrons ($(\mathbf{v}\times\mathbf{B})_{2\omega} = 0$)

Energy spectrum improvement for circular polarization

GEMINI laser, $\tau_p = 45$ fs, $I = 6 \times 10^{20}$ W cm^{-2}, 15 nm thick CH foils

- CP brings larger cut-off energies & spectral peaks for both species
- simulations: transparency-limited acceleration, proton spectrum not well reproduced

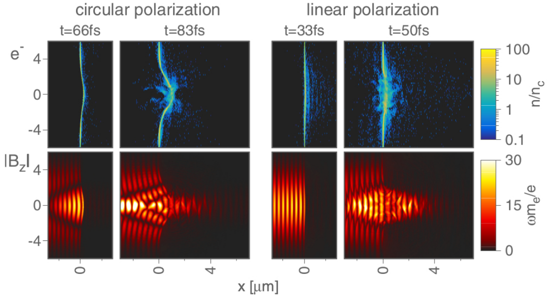

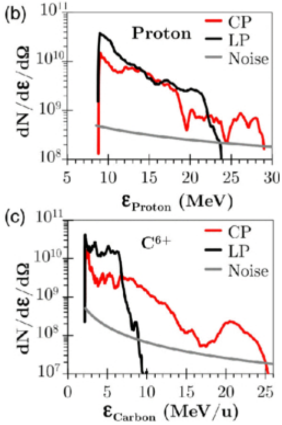

Scullion et al,
PRL **119** (2017) 054801

Beyond the mirror: charge separation effects

Real targets are not perfect rigid mirrors: local light pressure separates charges until electrostatic tension balances $P_{\rm L} = 2I/c$
Space-charge field E_x accelerates and bunches ions in the skin layer $(x_d < 0 < x_s)$ until "breaking" at $x = x_s$, $t = t_b$
("hole boring" acceleration)

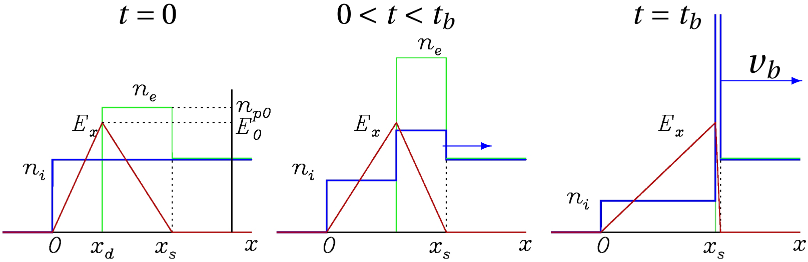

Macchi et al PRL **94** (2005) 165003

Hole boring modeling and dynamics

Simple model yields $\frac{v_b}{c} \simeq \left(\frac{Z m_e n_c}{A m_p n_e}\right)^{1/2}$ $\quad t_b \simeq \frac{c/\omega_p}{v_b}$

and velocity spectrum $0 < v_i < 2v_b$ $\quad$ (v_b: average front velocity)

PIC simulation: onset of electron heating at "breaking" ($t = t_b$)

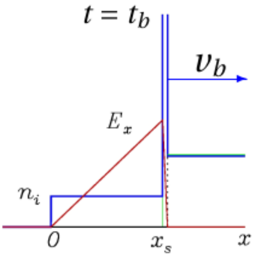

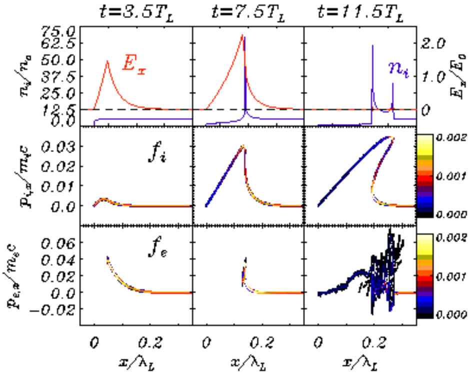

Hole boring: steady model

Snowplow model for "averaged" motion: "piston" reflection from the laser front
Balance of EM & kinetic momentum flow:

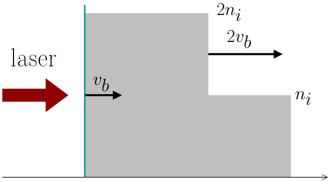

$$\frac{2I}{c}\frac{1-v_b/c}{1+v_b/c} = n_i\gamma_b(2m_i\gamma_b v_b)v_b$$

$$\frac{v_b}{c} = \frac{\Pi^{1/2}}{1+\Pi^{1/2}} \qquad \frac{\mathcal{E}_b}{m_p c^2} = \frac{2\Pi}{1+2\Pi^{1/2}} \qquad \Pi \equiv \frac{Zn_c m_e}{An_e m_p}a_0^2$$

A.P.R.Robinson et al. PPCF **51** (2009) 024004

- steady model allows relativistic generalization for v_b
- modeling of multispecies acceleration more difficult

From hole boring to light sail

With proper choice of thickness a single ion bunch can be produced and re-accelerated as laser front advances

Macchi et al, PRL **103** (2009) 85003;

New J. Phys. **12** (2010) 045013

Light Sail motion emerges as the average over multiple re-acceleration stages

Grech et al, New J. Phys. **13** (2011) 123003]

Multiple species complicate the picture!

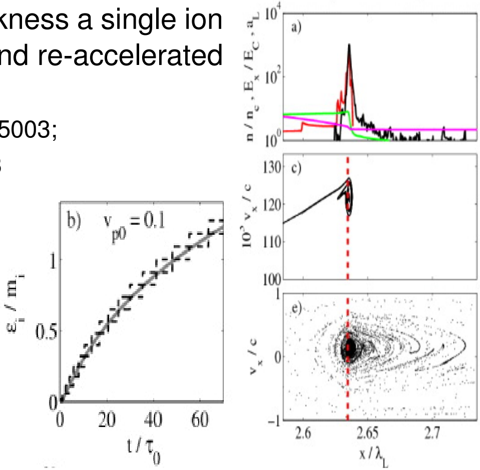

Multispecies effects

- For coherent light sail motion all species move with same V

$\longrightarrow$ ideally same energy/nucleon for each Z/A

- self-organized acceleration is complicated by multiple ion species (e.g. no simple self-similar motion & bunching)
- LS proton acceleration requires tight control of target thickness and species spatial distribution (experimentally challenging)

  [see e.g. Macchi et al PRL **103** (2009) 85003;

  Qiao et al PRL **105** (2010) 155002]

- Alternate "brute" strategy: remove impurity protons and aim at heavier ion acceleration

  McIlvenny et al PRL **127** (2021) 194801

Exploiting the prepulse: acceleration of Carbon ions

For 15 nm thickness
the energy/nucleon
is higher for C^{6+} ions
Simulating the ps prepulse
interaction shows removal of
impurity protons (H^+)

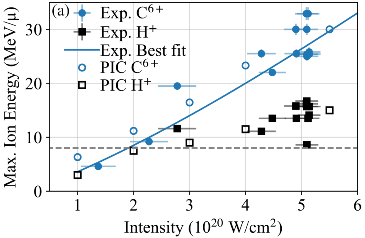

McIlvenny et al PRL **127** (2021) 194801

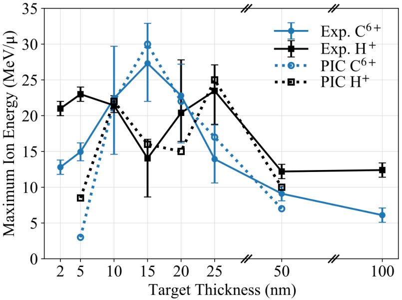

Energy scaling $\propto I^{1.2}$ still limited by transparency onset

GEMINI laser, $I = 4.5 \times 10^{20}$ W cm^{-2}, $\tau_p = 45$ fs, $2 - 100$ nm thick C foils with H impurities

Public coverage (FLASH-stimulated?)

physicsworld | **particle therapy**

PARTICLE THERAPY | RESEARCH UPDATE

Intense radiation pressure enables selective acceleration of carbon ion beams

07 Dec 2021

Physics Today **75**, 1, 19 (2022); https://doi.org/10.1063/PT.3.4916

Mirror

Irish boffins' laser to help beat cancer

A laser selectively kicks carbon out of a foil

Experiments and simulations show how the shape of a laser's profile determines which target atoms make up the resulting ion beam.

Physics

A New Trick to Make Short-Pulse Ion Beams

A new laser technique could lead to ultrashort-pulse, high-energy ion beams for medical use.

Light sail with foam-induced pulse shaping

Adding a low-density Carbon Nanotube Foam layer enables pulse steepening for spatio-temporal pulse steepening
$\longrightarrow$ faster push to gain energy before transparency and instability

Bin et al, PRL **115** (2015) 064801

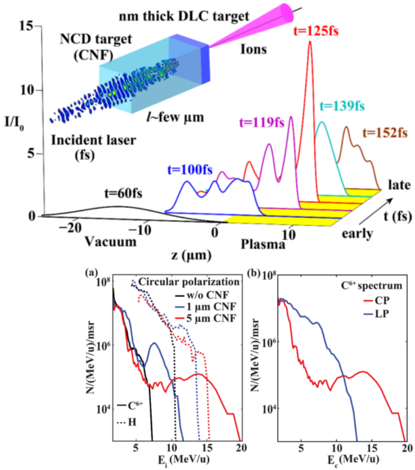

GEMINI laser

$I = 2 \times 10^{20}$ W cm^{-2},

$\tau_p = 45$ fs

Diamond-Like Carbon 10 nm foils

covered with CNF

Counteracting transparency with ionization buffer

Adding a heavy-ion layer (e.g. Au on Al) provides a reservoir of free electrons to the sail delaying the transparency onset

Shen et al, PRL **118** (2017) 204802

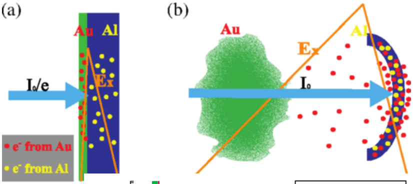

First experimental evidence:

Au layer improves spectral features

VULCAN laser, $I = 3 \times 10^{20}$ W cm^{-2},

$\tau_p = 850$ fs, CD targets

Alejo et al PRL **129** (2022) 114801

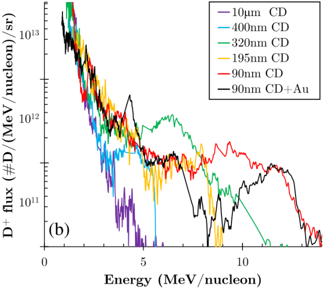

Extreme intensity: Light Sail “unlimited”?

- Transverse expansion of the target reduces surface density $\rho\ell$
- Decrease of laser frequency in “sail” frame delays the transparency onset

$\longrightarrow$ enhanced acceleration

at the expense of the number of ions

[S.V.Bulanov et al. “Unlimited ion acceleration by radiation pressure” PRL **104** (2010) 135003]

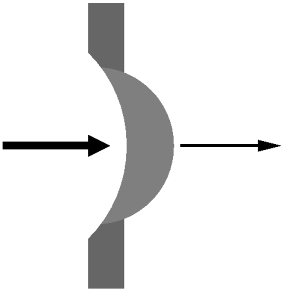

Energy gain in the relativistic regime is faster in 3D than in 1D:

$$\gamma(t) = \left(\frac{t}{\tau_k}\right)^k \qquad k = \frac{D}{D+2} = \begin{cases} 1/3 & (1D) \\ 3/5 & (3D) \end{cases}$$

Very tight focusing needed for “prompt” transverse boosting

Analytical model for multi-D Light Sail

Self-similar transverse dilatation $r_\perp(t) = \Lambda(t) r_\perp(0)$

$$\sigma = \sigma(t) = \frac{\sigma(0)}{\Lambda^{D-1}(t)}\,, \qquad \frac{\mathrm{d}}{\mathrm{d}t}(\gamma\beta_\parallel) = \frac{2I}{\sigma(0)c^2}\Lambda^{D-1}(t)\frac{1-\beta_\parallel}{1+\beta_\parallel} \qquad (D = 1,2,3)$$

Impulsive transverse kick by ponderomotive force

$$\frac{\mathrm{d}p_\perp(t)}{\mathrm{d}t} \simeq -m_e c^2 \partial_r (1 + a^2(r,t))^{1/2} \simeq 2 m_e c^2 a_0 r / w \qquad (a_0 \gg 1\,,\ r \ll w)$$

→ transverse momentum scales linearly with position

$$\frac{\mathrm{d}\Lambda}{\mathrm{d}t} = \frac{\dot{r}_\perp(t)}{\dot{r}_\perp(0)} = \frac{\alpha}{\gamma(t)}\,, \qquad \gamma(t) \simeq (p_\parallel^2 + m_i^2 c^2)^{1/2}\,, \qquad \alpha \simeq 2\frac{m_e a_0 c^2 \Delta t}{m_p w^2}$$

Solution in the $\gamma \gg 1$ limit $\quad \gamma = \left(\frac{t}{\tau_k}\right)^k, \quad k = \frac{D}{D+2}$

Fast scaling in 3D confirmed by simulations

Laser: 24 fs, 4.8 μm spot, $I = 0.85 \times 10^{23}$ W cm^{-2} $\Longrightarrow$ 1.5 kJ
Target: $d = 1$ μm foil, $n_e = 10^{23}$ cm^{-3}

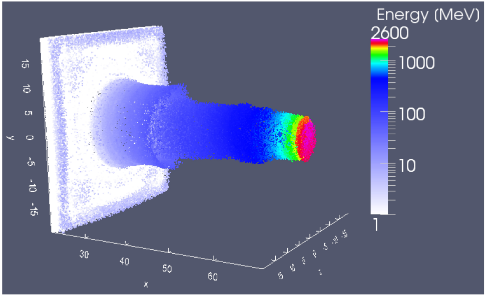

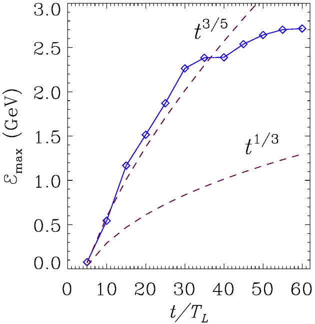

$\mathcal{E}_{\text{max}} \simeq 2.6$ GeV $>$ 4 X 1D prediction (still limited by transparency)
Sgattoni et al, Appl. Phys. Lett. **105** (2014) 084105

Light Sail Rayleigh-Taylor instability

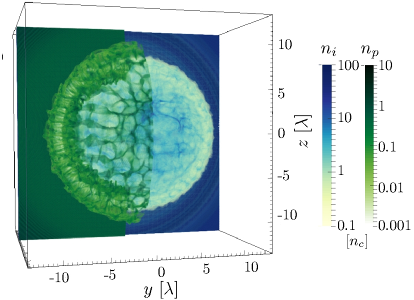

3D light sail simulation: formation of net-like structures with size $\sim \lambda$ (laser wavelength) and $\sim$ hexagonal shape

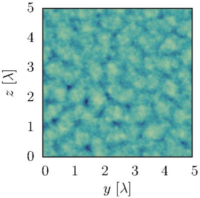

two-species target: H^+, C^{6+}

Interpretation: Rayleigh-Taylor instability driven by light pressure

Sgattoni et al, Phys. Rev. E **91** (2015) 013106

Rayleigh-Taylor Instability in space and lab

Crab Nebula (Hubble)

Heavy fluid
over a
light fluid
is unstable
(↑ gravity
↓ acceleration)

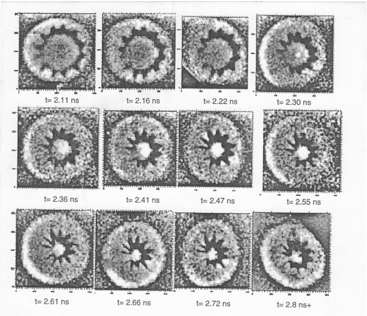

ICF implosion, 1995

Exagon formation in RTI is an example of “spontaenous symmetry breaking” in a classical system

S.I.Abarzhi, PRE **59** (1999) 1729

Plasmonic effects on RTI

The EM field at a rippled surface of spatial period d is modulated
The P-component is resonantly enhanced when $d \sim \lambda$ due to the excitation of surface plasmons

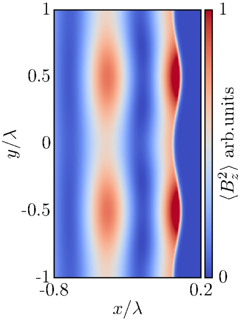

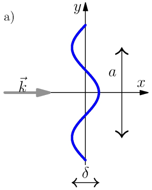

geometry

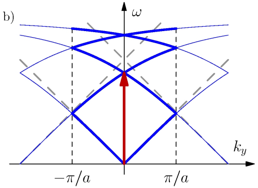

matching conditions

The resulting modulation of laser light pressure provides a spatial seed for RTI

Sgattoni et al,
PRE **91** (2015) 013106

Thin foil RTI with self-consistent pressure modulation

Model: reflection from shallow 2D grating of depth δ
+ modified Ott's theory [PRL **29** (1972) 1429]
with modulated pressure:

$$P \simeq P_0(1+K(q)\delta\cos qy)\,, \qquad K(q) = \begin{cases} -(q^2-k^2)^{1/2} & (S) \\ k^2 q(q^2-k^2)^{-1/2} & (P) \\ (k^2-q^2/2)(q^2-k^2)^{-1/2} & (C) \end{cases}$$

$$\gamma = (P_0/\sigma)^{1/2}\left[\left(q^2+K^2(q)/4\right)^{1/2} + K(q)/2\right]^{1/2}$$

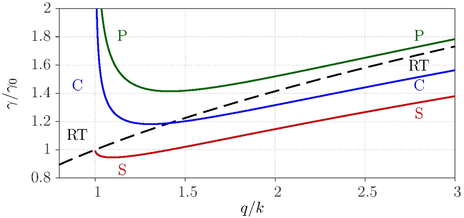

S-polarization
P-polarization
C-ircular polarization
RT: no modulation ($\delta = 0$)

Relativistically Induced Transparency Acceleration

Many effects contribute to RIT: target heating & expansion, 3D bending & rarefaction, instabilities . . .

PIC simulations (*) are necessary for a complete picture

RITA is a complex scenario: several acceleration mechanisms are activated and may cooperate to yield high energy ions (typically with broad spectra and maximum energy off-axis)

* Note: 3D is required for realistic predictions

3D PIC simulation of laser interaction with a thin target showing breakup to transparency
[A. Sgattoni, AlaDyn code]

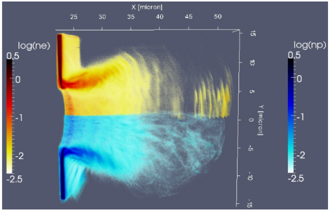

Example: >94 MeV protons from RITA

VULCAN laser, $I = 3 \times 10^{20}$ W cm^{-2}, $\tau_p = 900$ fs, plastic foil targets
Analysis based on simulations outlines a hybrid TNSA-RPA regime enhanced by magnetic collimation of fast electrons

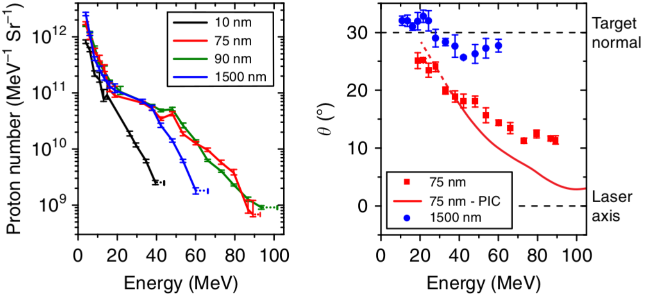

Higginson et al. Nature Comm. **9** (2018) 724

Heavy ions from RITA

CoReLS laser
$I = 1.1 \times 10^{22}$ W cm^{-2}, $\tau_p = 22$ fs
150 nm Au foil with & w/o
Carbon Nanotube Foam layer

TRIDENT laser, $I = 2 \times 10^{20}$ W cm^{-2}
$\tau_p = 650$ fs, 110 nm Al foil

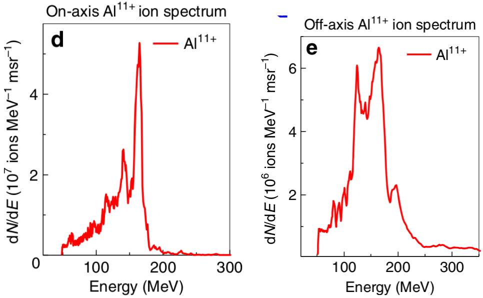

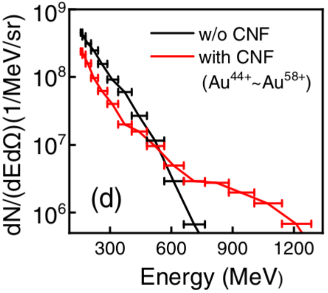

Palaniyappian et al. Nat. Comm. **9** (2018) 724

Wang et al. PRX **11** (2021) 021049

Collisionless Shock Acceleration

- Base: collisionless (*) shock wave of supersonic velocity $v_s = Mc_s$ $(M > 1,\ c_s = \sqrt{ZT_e/Am_p})$ (in)directly driven by the laser pulse

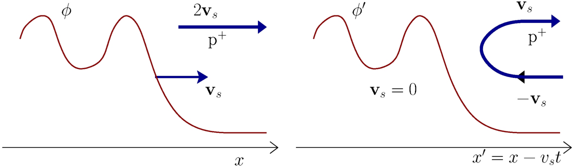

- Shock front is a moving potential barrier → *reflection* of *some* ions from the front: $v_i \simeq 2v_s$

→ acceleration of *monoenergetic*, multi–MeV ions if v_s is constant and $T_e \simeq T_{\text{pond}}$ at $a_0 > 1$

* sustained by a charge separation field rather than by collisions (viscosity)

CSA or Hole Boring RPA?

RPA/HB: laser-"piston" pushed surface motion at velocity v_b
+ bunch ions at velocity $2v_b$
$\longrightarrow$ often confused with "direct drive" CSA when $v_s \gtrsim v_b$

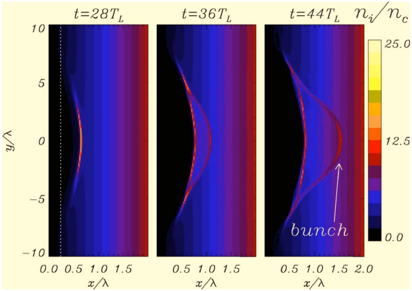

Basic differences:

- CSA occurs in plasma bulk (not at surface)
- number of accelerated ions in CSA strongly limited by shock loading
- RPA (CSA) favored by cold (hot) plasma & CP (LP) laser

Experiments with gas targets and CO_2 lasers:
RPA: Palmer et al, PRL **106** (2011) 14801
CSA: Haberberger et al Nat. Phys. **8** (2012) 95
Tresca et al PRL **115** (2015) 094802

Shock Loading and Energy Chirping

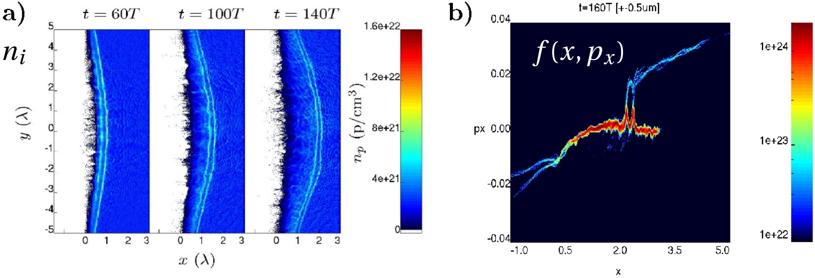

2D PIC simulation

Shock loses energy to ions → v_s decreases → ions velocity $(2v_s)$ decreases → spectrum broadens towards lower energies (monoenergetic only for very low ion flux)

(Very high resolution required in particle simulations!)

Macchi et al, PRE **85** (2012) 046402; Sgattoni et al, Proc. SPIE **8779** (2013)

(Hybrid) CSA in low-density targets

CS formation required low-density plasma:
$n_e \simeq n_c$ ("near-critical") as a compromise between good coupling and low collisionality
- gas targets (suitable for high repetition rate)
- preformed plasmas (exploiting prepulse/dual pulse)

Up to 45 MeV protons observed for prepulse-exploded foils in a hybrid CSA-TNSA scenario
Antici et al. Scient. Rep. **7** (2017) 16463
see also:
Zhang et al. PRL **119** (2017) 164801
Chen et al. Scient. Rep. **7** (2017) 13505

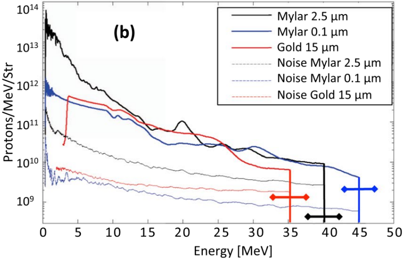

Cryogenic hydrogen targets: experiments

- Continous “flowing” target ⟶ high repetition rate
- moderate density ⟶ enhanced laser coupling
- pure hydrogen content ⟶ pure proton beam

Promising performance (comparable to TNSA) on several laser systems for both ribbon & cylindrical jet

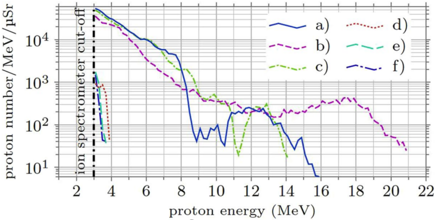

Polz et al. Scient. Rep. **9** (2019) 16534

see e.g.:
Obst et al. Scient. Rep. **7** (2017) 10248
Kraft et al. PPCF **60** (2018) 044010
Gauthier et al. APL **111** (2017) 114102

Cryogenic hydrogen targets: perspectives

Reduced density makes RPA-HB scaling promising

Example: 2D simulation

~ 5 fs, 10^{22} Wcm^{-2} pulse

$n_e = 50 n_c$ H jet

Macchi & Benedetti, NIMA **620** (2010) 41

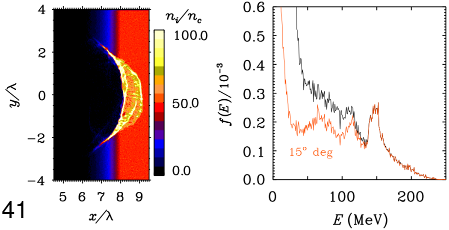

See also: Robinson et al, PoP **18** (2011) 056701 & PPCF **54** (2012) 115001

Psikal & Matys PPCF **60** (2018) 044003

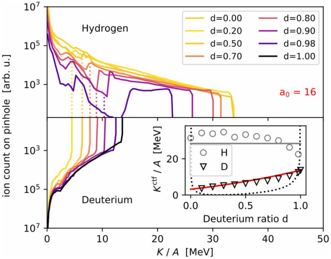

Extended simulation study suggests exploting multispecies effect in H-D jet

Huebl et al. PPCF **62** (2020) 124003

A note: use simulations with care

The cut-off energy may be strongly overestimated in 1D/2D (particularly relevant for TNSA & RITA)

PIC simulations of TNSA w/o foam layer
Sgattoni et al, PRE **85** (2012) 036405
see also: Stark et al, PoP **24** (2017) 053103
d'Humières et al, PoP **20** (2013) 023103;

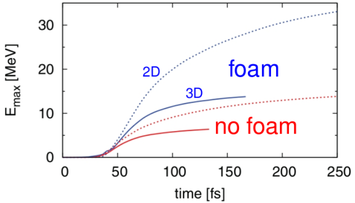

Results may be affected by limited numerical resolution

1D simulation of CSA: "continuous" no-noise Vlasov shows differences with PIC even at 10^3 part/cell and $\Delta x = 10^{-3}\lambda$
Grassi et al, PPCF **58** (2016) 034021

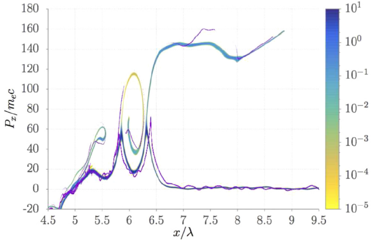

Conclusions & Outlook

Temporary page!

LaTeX was unable to guess the total number of pages correctl
As there was some unprocessed data that should have been
added to the final page this extra page has been added to
receive it.
If you rerun the document (without altering it) this surplus pa
will go away, because LaTeX now knows how many pages to
expect for this document.